Dynamic Light Scattering and Dynamic Viscoelasticity of Poly(vinyl alcohol) in Aqueous Borax Solutions. 5. Temperature Effects

Kazuki Koga, Akihiko Takada, and Norio Nemoto*

Department of Molecular and Material Sciences, IGSES, Kyushu University, Hakozaki, Fukoka 812-8581, Japan

Received April 5, 1999; Revised Manuscript Received October 19, 1999

ABSTRACT: Steady viscosity, dynamic viscoelasticity (DVE), and dynamic light scattering (DLS) measurements were made to study the effects of temperature, T, on association behaviors of poly(vinyl alcohol) (PVA) with weight-average degree of polymerization $DP_w = 350$ in aqueous Borax solution. Intrinsic viscosity, $[\eta]$, monotonically decreased by 23% with a rise in T from 10 to 65 °C. At low T, enhancement in viscosity was observed with increasing polymer concentration, C, due to formation of viscoelastic network with the didiol complex as temporal cross-links, and the time−temperature superposition principle was found to be applicable for construction of a composite curve at each C. Those composite curves were further reduced so as to give one master curve. The system tended to lose its viscoelastic nature, when raising the temperature, toward a viscous solution owing to a decrease in the number of the didiol complexes as well as the shrinkage of the PVA chains. We found from analysis of DVE and DLS data that a clear boundary line between viscoelastic and viscous behaviors can be drawn on the $T-C$ diagram using the temperature T_N defined as the inflection point in a η vs T^{-1} plot for each C.

Introduction

In previous reports,[1−4] we studied dynamics of aqueous solutions of poly(vinyl alcohol) (PVA)/borax using dynamic light scattering (DLS) and dynamic viscoelasticity (DVE) techniques. The most remarkable finding obtained from those experiments were the presence of the threshold concentration C_N at which a suspension of huge clusters, being composed of PVA chains interconnected to each other through formation of the didiol complexes, rather abruptly transformed to a temporarily cross-linked viscoelastic network. From intrinsic viscosity measurements and also an empirical relation between C_N and the weight-average molecular weight M_w found as $C_N \sim M_w^{-0.5}$, we concluded that PVA chains took the unperturbed dimension at C_N irrespective of M_w, and that C_N was very close to the overlapping concentration C^* conventionally defined as $C^* = 1/[\eta]\rho_{sp}$ where $[\eta]$ and ρ_{sp} are intrinsic viscosity and specific density of PVA, respectively.

Complexation of Borax with hydroxyl-containing polymers have been extensively studied using ^{11}B NMR spectroscopy for poly(vinyl alcohol),[5−7] poly(saccharide)s,[7,8−10] poly(glyceryl methacrylate),[9] and cellulose derivatives.[11,12] Those studies have revealed that the didiol complex is in chemical equilibrium with boric acid, borate anion, and the monodiol complex, and that the number density of the didiol complex decreases with increasing temperature T accompanied by shortening of its lifetime τ_0. Then, it does not seem unreasonable to suppose that a viscoelastic network with $C > C_N$ smoothly changes to a viscous solution with increasing T. As a matter of fact, we observed that PVA/Borax samples became transparent solutions with low viscosity when heated to 80 °C, being homogeneous in appearance. In part 1 of this series, we also studied effects of temperature on dynamical behaviors of the 2.0 wt % PVA/Borax solution prepared from the PVA sample with the degree of polymerization $DP = 1750$ and the degree of saponification of 96.0 mol % over the T range from 25.0 to 40.0 °C. DLS and DVE data showed that such the transition did not take place in this narrow T range, and that the viscoelastic network was preserved in such a manner that the relaxation time τ_M characteristic of the network decreased and the dynamical correlation length ξ_H slightly increased with increasing T, which may be interpreted as being due to a decrease in the number as well as shortening of the lifetime of the transient cross-linking points.

The above argument is, however, rather intuitive and may not hold for the PVA/Borax system for a couple of reasons. First, PVA is a neutral polymer and soluble in water due to favorable interaction with water, i.e., by formation of hydrogen bonds between hydroxyl residues and water molecules. Strength of hydrogen bonding becomes weaker with increasing T so that water may become a poor solvent to a PVA chain at higher T. This tendency may be accelerated whenever the degree of saponification is not 100% and a considerable number of hydrophobic acetate residues are present as side chains for test PVA samples. In this case, a decrease in the coil dimension of PVA molecules results in a shift of the threshold concentration C_N to higher concentration with increasing T. Second, the monodiol complexes endow polyelectrolyte nature to PVA chains. However, this effect is likely to diminish with increasing T. Third, an increase in free borate ions with T tends to screen electrostatic interaction so that the salt-out effect may induce aggregation of PVA chains. Thus, effects of temperature on structures and dynamics of the PVA/Borax system seem quite complicated.

In this paper, we present results of dynamic viscoelasticity(DVE), dynamic light scattering (DLS) measurements on aqueous Borax solutions of PVA with weight-average degree of polymerization $DP_w = 350$ and polymer concentrations C ranging from 3.0 to 7 wt % over a wide range of temperature. We also report an

* To whom correspondence should be addressed.

10.1021/ma990493w CCC: $18.00
Published on Web 12/03/1999

effect of T on the coil dimension from intrinsic viscosity measurements. We shall show that all dynamic viscoelastic data can be reduced to one master curve which systematically describes the whole aspect of DVE behaviors of the PVA/Borax system as functions of T and C, and we propose, though quite empirically, that the temperature T_N defined as the inflection point in a η vs T^{-1} plot for each C may be a useful parameter along with C_N for understanding dynamics of this system.

Experimental Section

Materials. In this study, we have chosen the lowest molecular weight sample of poly(vinyl alcohol) (PVA) used in earlier investigations.[2−4] The weight-average degree of polymerization DP_w is 350 with the molecular weight distribution of $M_w/M_n = 2.60$ and the degree of saponification of 88.0 mol %, which were characterized by the supplier(Kurary Co., Ltd). Concentrated stock solutions of PVA and of sodium borate (SB), $Na_2B_4O_7 \cdot 10H_2O$, were prepared separately using dust-free purified water and made optically clean by filtration with a Millipore filter (nominal pore size, 0.20 μm). Prescribed amounts of the two solutions were poured into the sample cell to obtain seven solutions with PVA concentration C ranging from 3.0 to 7.0 wt %. The SB concentration was always adjusted to half of the PVA concentration by weight. Finally, the cell was rotated at 0.2 rpm for about 2 h at 80 °C in order to make samples homogeneous and transparent. The sample code PVAX-Y represents DP_w as X and C as Y in weight percent for the PVA/SB solutions tested.

Methods. The intrinsic viscosity of the PVA sample in aqueous solution was measured with an Ubbelohde type of capillary viscometer over a range of temperature from 10 to 65 °C. Dynamic viscoelastic (DVE) measurements were made with a stress-controlled rheometer (CLS100, Carri-MED, ITS Japan) using a parallel plate geometry with a diameter of 4 cm. The complex shear modulus was found to be independent of the strain applied when the strain was less than 0.7. The storage and the loss shear moduli, $G'(\omega)$ and $G''(\omega)$, of the samples were measured at a strain of 0.3 over an angular frequency, ω, from 0.01 to 100 rad/s at eight temperatures T = 10, 15, 25, 35, 45, 55, 65, and 75 °C. A humidity chamber was used to prevent solvent evaporation. The steady-state shear viscosity of the solutions which possessed viscosity lower than that estimated from DVE measurements but higher than that measured by the capillary viscometer was measured with the same geometry as used for the dynamic viscoelastic measurements with a shear rate sufficiently lower than the shear rate at which shear thickening occurs.

Dynamic light scattering(DLS) measurements were made with a spectrometer(ALV-125) equipped with a multiple-τ digital correlator (ALV-5000FAST). A vertically polarized single frequency 488 nm line of an argon ion laser (Spectra Physics, Beamlock 2060) was used as a light source with an output power of 330 mW. The normalized time correlation function, $A_q(t)$, of the vertical component of the light intensity scattered from three PVA/Borax samples with C = 3.8, 4.2, and 4.5 wt % was measured over a range of the scattering angle θ from 15 to 150° at T = 15, 25, 35, 45, and 65 °C.

We performed all measurements within 1 or 2 days after sample preparation. Repeated DVE and DLS measurements after the first run gave the same results at room temperature, indicating that PVA molecules did not suffer from any damage by heating to 75 °C.

Results

Intrinsic Viscosity. Solution viscosity η of the PVA sample in dilute aqueous Borax solutions with a constant weight ratio of PVA/SB = 2:1 was measured at seven temperatures T ranging from 10 to 65 °C. Conventional plots of η_{sp}/C and $\ln \eta_r/C$ against polymer concentration C were expressed by straight lines with positive slopes in the dilute regime of $C < 0.01$ g/mL.

Table 1. Values of $[\eta]$ and C^* at Seven Temperatures

T/°C	$[\eta]/10^3$mL g^{-1}	C^*/wt %
10	26.1 ± 0.4	3.62
15	27.0 ± 0.5	3.51
25	24.4 ± 0.4	3.63
35	24.9 ± 0.4	3.79
45	23.1 ± 0.2	4.07
55	22.3 ± 0.4	4.2
65	20.2 ± 0.2	4.61

Intrinsic viscosity $[\eta]$ was estimated from linear extrapolation of the data to infinite dilution to an experimental accuracy of 1.5% As is evident from $[\eta]$ values listed in Table 1, $[\eta]$ monotonically decreases with an increase in T from 25 to 65 °C by more than 20%. In a previous report,[4] we showed that water is a good solvent to PVA at T = 25 °C from the molecular weight dependence of $[\eta]$ and also that a PVA molecule with low molecular weight such as $DP_w = 350$, nevertheless, took the unperturbed dimension, which is not inconsistent with the trend that $[\eta]$ asymptotically approaches to a constant value of 0.26 ± 0.01 g/mL below room temperature. We also showed that addition of sodium borate did not affect the $[\eta]$ value of this PVA molecule. Therefore, the noticeable decrease in $[\eta]$ with T should be attributed to the point that the strength of hydrogen bonding between water and hydroxyl groups of PVA becomes more and more weak with a rise in T, so that water may be considered as a poor solvent at sufficiently high T and is likely to cause shrinkage of PVA chains.

As stated in the Introduction, C_N at which a viscoelastic network is formed was found to be very close to the overlapping concentration C^* calculated as $C^* = 1/[\eta]\rho_{sp}$. As listed in Table 1, C^* becomes higher with T, thus the shrinkage of a PVA chain may result in a shift of C_N to higher concentration with increasing T. The temperature effect on the chain dimension will be discussed more in detail later.

Dynamic Viscoelasticity(DVE). We attempted to measure the storage and the loss shear moduli, $G'(\omega)$ and $G''(\omega)$, over a T range from 10 to 75 °C for all solutions but were successful only in a limited T range. Figure 1 illustrates angular frequency ω dependencies of $G'(\omega)$ and $G''(\omega)$ for PVA350−7.0 with the highest C among the samples tested in this work. In the figure, G' and G'' at respective temperatures are shifted along the vertical axis by multiplying 10^n with n values, as indicated in the figure, to prevent data overlapping.

G' and G'' are proportional to ω^2 and ω in the low ω region at six temperatures measured, respectively, which are characteristic behaviors of a viscoelastic network in the flow region as given by $G'' = \eta\omega$ and $G' = J_e\eta^2\omega^2$.[13] The steady viscosity η and the steady-state compliance J_e can be easily estimated from respective slopes, and the mechanical relaxation time τ_M is also conveniently evaluated as $\tau_M = J_e\eta$. The sample behaved as viscous fluid at T = 65 and 75 °C; thus, only η was estimated at these two temperatures. PVA/Borax solutions with lower C exhibited viscoelasticity in a narrower T range. Values of η, J_e, and τ_M are listed in Table 2.

We first attempted to superpose the G' and G'' data of each solution at different temperatures by the horizontal shift alone, but the attempt was unsuccessful as anticipated. All data could be successfully superposed by applying both the vertical and the horizontal shifts. Figure 2 shows two composite curves for PVA350-7.0 and PVA350-4.2 at the reference temperature T_r = 15

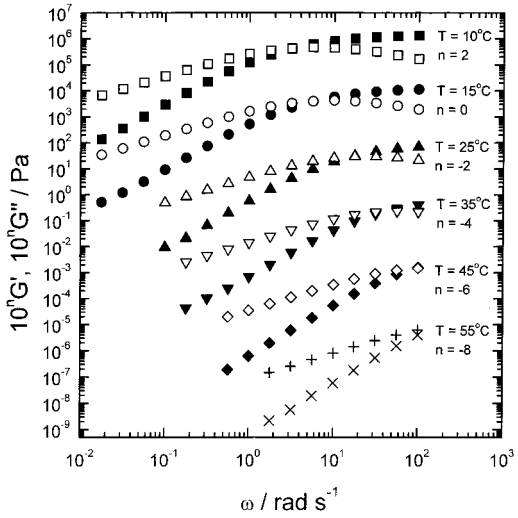

Figure 1. The storage and the loss shear moduli, $G'(\omega)$ and $G''(\omega)$, of a PVA/Borax solution with $C = 7.0$ wt % plotted against angular frequency ω at six temperatures from 10 to 55 °C. The data at respective temperatures are shifted along the vertical axis by multiplying 10^n with n values, as indicated in the figure, to avoid data overlapping. Symbols: filled ones and (×) for $G'(\omega)$ and unfilled ones and (+) for $G''(\omega)$.

°C as examples. Values of the horizontal shift factor, a_T, and the vertical shift factor, b_T, used for construction of composite curves, are given in Table 2.

We argued in previous reports[1−4] that ω dependencies of $G'(\omega)$ and $G''(\omega)$ at 25 °C for low molecular weight PVA/Borax solutions with $C > C_N$ could be closely represented by the Maxwell model with a single relaxation time. We found that composite curves in Figure 2 could be only approximately represented by the same model, and the best fit was obtained using eq 1, which assumed the presence of two relaxation modes. The results are shown by solid curves for each composite curve in Figure 2.

$$G'(\omega) = \sum_{i=1}^{2} \frac{G_i \omega^2 \tau_i^2}{1 + \omega^2 \tau_i^2}, \quad G''(\omega) = \sum_{i=1}^{2} \frac{G_i \omega \tau_i}{1 + \omega^2 \tau_i^2} \quad (1)$$

The composite curve was successfully constructed for solutions with other C. Values of G_i and τ_i ($i = 1, 2$) used for fitting are listed in Table 2, which indicates that τ_1 is longer than τ_2 by nearly 1 order of magnitude, while corresponding mechanical strengths are comparable. Values of J_e calculated from a phenomenological relation,[13] $J_e = \sum G_i \tau_i^2 / (\sum G_i \tau_i)^2$, agree with those given in Table 2 as expected. Obviously τ_1 and τ_2 both increase with polymer concentration. Thus, even the short relaxation time τ_2 less than 100 ms cannot be directly related to the lifetime of the didiol complex. In the earlier report,[4] we calculated the longest relaxation time $\tau_{R,1}$ of the Rouse model using eq 2, where η and η_s are

$$\tau_{R,1} = 6(\eta - \eta_s)M/\pi^2 CRT \quad (2)$$

viscosities of the solution and the solvent, respectively, and R is the gas constant. $\tau_{R,1}$ is found to be shorter than τ_2 by more than an order of magnitude at $C = 4.0$ and 5.0 wt % and shorter by a factor of 2 at $C = 7.0$ wt %. Thus, it is unlikely that the fast relaxation mode represents conformational relaxation of the PVA chain in the network. Success of time−temperature reduction, nevertheless, strongly suggests that molecular motions for the two modes are governed by the same relaxation mechanism.

The horizontal shift factors a_T of respective solutions are semilogarithmically plotted against the reciprocal of T in Figure 3. Here each a_T is shifted along the vertical axis by multiplying 10^n to prevent data overlapping with n values given in the figure. Log a_T data at higher C look linearly dependent on T^{-1} with slopes very slightly dependent on C, which indicates that the relaxation time follows the Arrhenius type of T dependence with almost the same activation energy ΔH. The activation energy ΔH from the slopes is 80 ± 5 kJ mol^{-1} in average, and is much larger than the value of $\Delta H = 40$ kJ mol^{-1} reported by Schultz and Myers[14] for aqueous Borax solutions of 100% saponified PVA with weight-average molecular weight $M_w = 112\,000$. The difference might be attributed to a fact that saponification of our PVA sample is 88%. When the forced linear fit are made to log a_T data at lower C, it appears that ΔH surely increases with decreasing C. This agrees with a finding of Ide et al.[12] that dynamic viscoelastic data of short-chain *o*-(2,3-dihydroxypropyl)cellulose in aqueous Borax solutions at various temperatures can be superposed to each other by applying both horizontal and vertical shifts and that the activation energy obtained from log a_T vs T^{-1} plots monotonically decreases with increasing polymer concentration.

The vertical shift factor b_T may reflect a change in the plateau modulus $G_N = G_1 + G_2$ with T. We estimated the number of elastically effective chains ν_{eff} from G_N using a equation of rubber elasticity $G_N = \nu_{eff} k_B T$ where the front factor was assumed to be equal to unity. Figure 4 gives a plot of log ν_{eff} against T^{-1}. Since data points are limited, we cannot give a definite conclusion. However, it appears that the T dependence of ν_{eff} closely follows the Arrhenius type equation with almost the same activation energy for $C < 7.0$ wt %. This result is once again in agreement with that for *o*-(2,3-dihydroxypropyl)cellulose by Ide et al.

Zero shear viscosity was measured for solutions to which dynamic viscoelastic response was not observed. We show temperature dependence of viscosity η obtained from flow measurements and also from dynamic viscoelastic measurements by the semilogarithmic plot of η against T^{-1} in Figure 5. Here η values in the dilute region of $C < 2.0$ wt % measured with an Ubbelohde type of viscometer are also shown, for comparison, to demonstrate that they are as low as on the order of 10^{-4}−10^{-5} Pa s and weakly dependent on T. The η of solutions with $C < 3.6$ wt % remains on the order of 10^{-3} Pa s at high temperatures and rapidly increases at the low T end. On the other hand, an enormous increases in η with T^{-1} are observed for solutions with higher C by nearly 4 orders of magnitude. In this case, the curves look to take a sigmoidal shape, which has been noticed for concentration dependence of η of the same PVA/Borax solutions with various degrees of polymerization DP_w from 350 to 3250 at constant temperature of 25 °C. The concentration at the inflection point in respective curves has been taken as the threshold concentration C_N at which viscous fluid rather abruptly transforms to a viscoelastic network and the composite curve could be constructed by plotting η of five solutions with different DP_ws against C/C_N. The same procedure was found to be applicable for superposition of η vs T^{-1} curves when we could locate the characteristic temperature T_N as the inflection point in

Table 2. Results of Dynamic Viscoelastic Measurements

sample code	T/°C	η/Pa s	J_e/Pa^{-1}	τ_M/s	a_T	b_T	τ_1/s	G_1/Pa	τ_2/s	G_2/Pa	G_N/Pa	ν_{eff}/mol m^{-3}	a_C	b_C
PVA350-3.6	10	1.6 ± 0.1	0.035	0.057 ± 0.006	2.4	0.56								
PVA350-3.6	15	0.418 ± 0.007	0.057	0.024 ± 0.004	1	1								
PVA350-3.8	10	8.4 ± 0.3	0.010	0.084 ± 0.001	2.3	0.58	0.11	60	0.025	90	150 ± 10	0.064		
PVA350-3.8	15	2.2 ± 0.1	0.017	0.037 ± 0.004	1	1	0.48	34.7	0.11	52			0.38	8.5
PVA350-4.0	10	28 ± 1	0.0045	0.13 ± 0.06	2	0.63	0.16	150	0.03	200	350 ± 20	0.15		
PVA350-4.0	15	8.6 ± 0.05	0.0071	0.063 ± 0.002	1	1	0.079	94	0.015	130			0.58	3.6
PVA350-4.0	25	0.65 ± 0.05	0.018	0.012 ± 0.002	0.2	2.9	0.015	32	0.0028	43				
PVA350-4.2	10	66 ± 2	0.0024	0.16 ± 0.023	1.7	0.71	0.19	250	0.035	420	670 ± 50	0.28		
PVA350-4.2	15	22 ± 3	0.0036	0.08 ± 0.02	1	1	0.11	170	0.020	290	470 ± 50	0.2	0.74	1.5
PVA350-4.2	25	2.1 ± 0.2	0.010	0.022 ± 0.005	0.25	2.6	0.028	68	0.0050	120				
PVA350-4.5	10	130 ± 5	0.0016	0.22 ± 0.02	1.8	0.83	0.22	450	0.045	500	1000 ± 150	0.42		
PVA350-4.5	15	51 ± 4	0.0023	0.12 ± 0.01	1	1	0.12	380	0.025	420	800 ± 100	0.33	1	1
PVA350-4.5	25	8 ± 0.05	0.0042	0.034 ± 0.005	0.29	2.1	0.035	180	0.0071	200				
PVA350-4.5	35	0.83 ± 0.01	0.011	0.009 ± 0.0005	0.086	5.2	0.010	72	0.0021	81				
PVA350-5.0	10	355 ± 8	0.00090	0.32 ± 0.04	1.7	0.91	0.35	800	0.06	1400	2200 ±200	0.93		
PVA350-5.0	15	180 ± 10	0.0011	0.2 ± 0.06	1	1	0.21	710	0.035	1200	1800 ± 170	0.75	1.4	0.38
PVA350-5.0	25	36 ± 1.5	0.0014	0.05 ± 0.01	0.31	1.6	0.063	450	0.011	790	1200 ± 300	0.48		
PVA350-5.0	35	4.9 ± 0.3	0.0033	0.016 ± 0.004	0.1	3.8	0.018	220	0.0031	390				
PVA350-5.0	45	0.63 ± 0.01	0.0083	0.005 ± 0.0003	0.012	10	0.0018	80	0.00031	140				
PVA350-5.5	10	880 ± 30	0.00060	0.53 ± 0.1	1.9	0.83	0.5	1600	0.08	1800	3400 ± 400	1.4		
PVA350-5.5	15	440 ± 25	0.00064	0.28 ± 0.01	1	1	0.27	1300	0.042	1500	2600 ± 400	1.1	2.2	0.3
PVA350-5.5	25	90 ± 5	0.00096	0.085 ± 0.01	0.3	1.7	0.080	800	0.013	900	2200 ± 500	0.69		
PVA350-5.5	35	18 ± 0.8	0.0016	0.028 ± 0.06	0.1	2.8	0.026	480	0.0042	550				
PVA350-5.5	45	3.8 ± 0.1	0.0032	0.012 ± 0.02	0.042	5.5	0.011	240	0.0018	270				
PVA350-5.5	55	0.3 ± 0.01	0.012	0.0036 ± 0.0005	0.013	8.3	0.0034	160	0.00054	180				
PVA350-7.0	10	3600 ± 150	0.00028	1.0 ± 0.16	1.7	0.91	0.7	5000	0.085	8500	13500 ± 500	5.7		
PVA350-7.0	15	2000 ± 80	0.00025	0.5 ± 0.1	1	1	0.41	4600	0.050	7800	12000 ± 1000	5.3	2.9	0.073
PVA350-7.0	25	510 ± 15	0.00027	0.14 ± 0.02	0.34	1.4	0.13	3900	0.015	6600	10000 ± 4000	3.5		
PVA350-7.0	35	150 ± 10	0.00026	0.05 ± 0.01	0.11	1.6	0.047	2700	0.0057	4700		2.9		
PVA350-7.0	45	35 ± 2	0.00044	0.015 ± 0.002	0.042	2.4	0.018	2000	0.0021	3300				
PVA350-7.0	55	7.8 ± 1.5	0.00077	0.006 ± 0.001	0.017	4.5	0.007	1000	0.00085	1700				

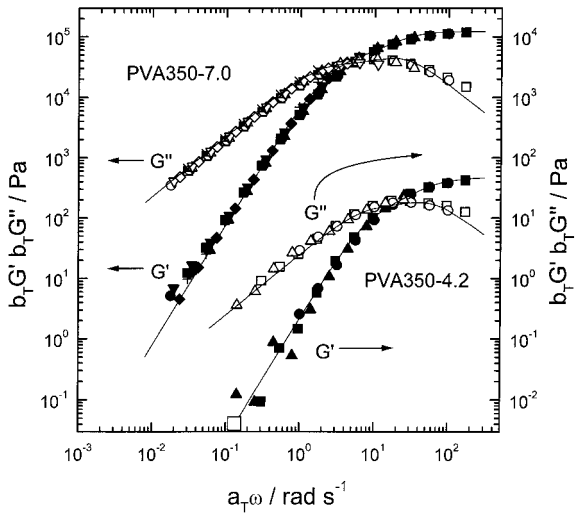

Figure 2. Time−temperature superposition principle applied for $G'(\omega)$ and $G''(\omega)$ data of the solution with $C = 7.0$ wt % in Figure 1. The composite curve for the solution with $C = 4.2$ wt % is also shown as an example. The reference temperature T_r is chosen 15 °C.

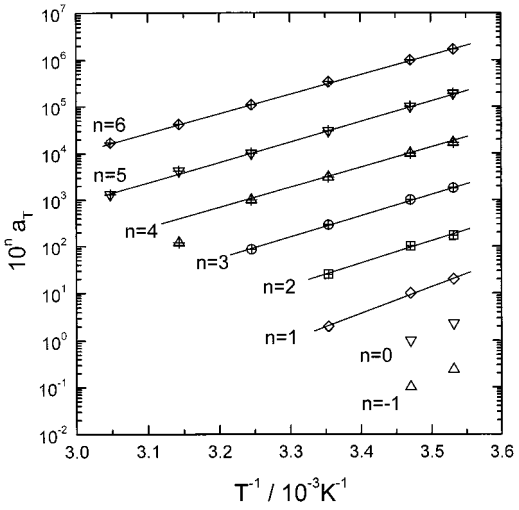

Figure 3. Semilogarithmic plot of the shift factor a_T against T^{-1}. Each a_T is shifted along the vertical axis by multiplying 10^n with n values, as indicated in the figure, to avoid data overlapping. Symbols for C (wt %; from top to the bottom): (cross in diamond) 7.0; (cross in down triangle) 5.5; (cross in up triangle) 5.0; (⊕) 4.5; (⊞) 4.2; (◇) 4.0; (▽) 3.8; (△) 3.6.

respective curves, though T_N was subjected to a considerable uncertainty. This will be discussed more in detail later.

Dynamic Light Scattering (DLS). We performed DLS experiments on three PVA/Borax solutions in a T range from 15 to 65 °C. Typical time profiles of the time correlation function $A_q(t)$, of the vertical component of the light intensity scattered from the solutions are given at two temperatures of 35 and 45 °C for solution with $C = 4.2$ wt % at scattering angles $\theta = 20$, 45, and 120° in parts a and b of Figure 6, respectively. The $A_q(t)$ exhibits the presence of two dominant decaying modes at both temperatures. The decay rate Γ_f characteristic of the fast decaying mode for the solution with $C = 4.2$ wt % was found to be proportional to the square of the magnitude of the scattering vector **q** at all temperatures measured, i.e., being independent of whether the solution exhibited viscoelasticity or not at respective temperatures. The q^2 dependence of Γ_f was also satisfied for other two solutions with C = 3.8 and 4.5 wt %. We estimated the dynamical correlation length ξ_H using the Stokes−Einstein relation (eq 3), as given in Table 3.

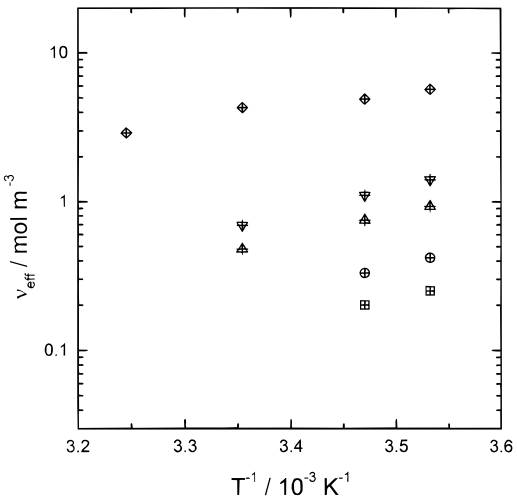

Figure 4. Semilogarithmic plot of the number of elastically effective chains ν_{eff} calculated from the plateau modulus G_N against T^{-1}. Symbols are the same as in Figure 3.

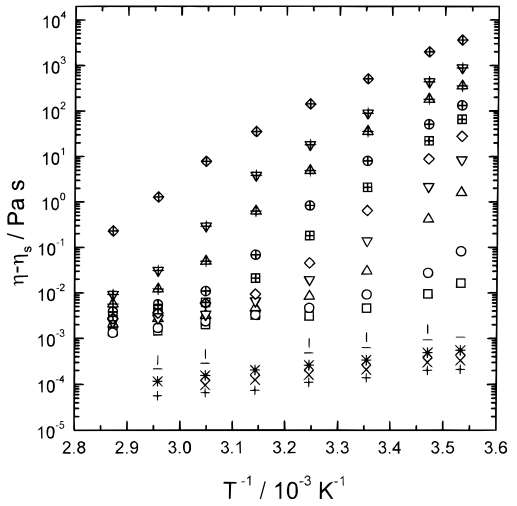

Figure 5. Semilogarithmic plot of the steady viscosity $\eta - \eta_s$ against T^{-1}. Symbols are the same as in Figure 3 for C from 7.0 to 3.6 wt %. Additional symbols for C values (wt 5%): (○) 3.3; (□) 3.0; (|) 2.0; (−) 1.5; (∗) 1.0; (×) 0.7; (+) 0.5 wt %.

$$\xi_H = \frac{q^2 k_B T}{6\pi\eta_s \Gamma_f} \tag{3}$$

Here k_B and η_s are the Boltzmann constant and the solvent viscosity, respectively. From Table 3, ξ_H is likely to increase gradually with T in the T range from 15 to 65 °C where we observed transformation of the solutions from viscoelastic networks to viscous fluids. The monotonic change in ξ_H with T is in contrast with C dependence of ξ_H to which a stepwise change took place at C_N.[4] The ξ_H represents a spatial scale of local concentration fluctuation related to the cooperative diffusive motion which becomes detectable by DLS whenever C exceeds the overlapping concentration $C^* = 1/[\eta]\rho_{sp}$.[15,16] In taking into account C^* values listed in Table 1, chain overlapping may not occur in two solutions with low C values at higher T. In our case that PVA chains are physically cross-linked by didiol complexes; alternatively, ξ_H may be also considered as representing a mesh size of the network. The number of the didiol complexes surely decreases with increasing T, which is not inconsistent with a gradual increase in ξ_H with T. Another possibility is that the solutions do not immediately become molecular solutions but contain a large number of huge clusters, and then ξ_H may be related to local molecular motions inside the clusters.

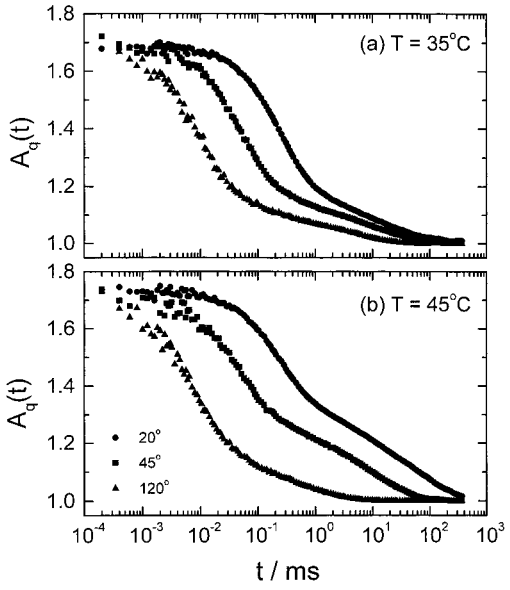

Figure 6. Time correlation function $A_q(t)$ of the vertical component of light intensity scattered from the solution with $C = 4.2$ wt % at three scattering angles $\theta = 20$, 45, and 120° at (a) $T = 35$ and (b) 45 °C.

Shibayama et al. performed small-angle neutron scattering measurements on the same PVA/Borax system under an alkaline condition.[17] The DP of resaponified PVA was 120, and concentrations of two samples were 12.5 and 16.7 wt %. They found that a gel−sol transition gave rise to variation of the correlation length ξ. The ξ remained constant in the gel state at around 11 nm and decreased steeply with increasing T in the sol state. Their result disagrees with our result, to which we have no explanation.

Figure 7 shows the scattering vector dependence of the decay rate Γ_s characteristic of the slow mode at five different temperatures for the solution with $C = 4.2$ wt %. Obviously, two types of q dependence are observed; at three lower T values of 15, 25, and 35 °C, Γ_s takes a constant value over the whole q range measured and Γ_s^{-1} agrees with τ_M obtained from DVE measurements for the same sample, so that the slow mode must be the relaxation mode. As extensively discussed in an earlier report,[1] such a behavior can be interpreted as being due to dynamical coupling between concentration fluctuation and elastic stress of network[18−20] and taken as evidence that a stable viscoelastic network is being formed for the PVA/Borax solution with $C = 4.2$ wt % in this T range. On the other hand, Γ_s becomes proportional to q^2 at $T = 45$ and 65 °C; i.e., the mode is the diffusive one. It is to be noted that the solution behaves as viscous fluid above 45 °C. It seems reasonable to suppose that the solution is depicted as a suspension of clusters whose internal motions are reflected in ξ_H. Assuming that clusters are spherical ones, we can calculate the average radius of the cluster, R, instead of ξ_H using eq 3 and Γ_s/q^2. The value of R is calculated as 83 and 96 nm at $T = 45$ and 65 °C, respectively, when values of solution viscosity at respective T are substituted for η_s. Values of Γ_s and R are summarized in Table 3. Use of water viscosity in eq 3 gave unphysical values on the

Table 3. Results of Dynamic Light Scattering Measurements

sample code	T/°C	D_f/nm^2 s^{-1}	ξ_H/nm	Γ_s/s	$D_s/10^5$ nm^2 s^{-1}	R/nm
PVA350-3.8	10	6.3 ± 0.5	2.5 ± 0.2	12 ± 2		
PVA350-3.8	15	6.8 ± 0.8	2.7 ± 0.2	30 ± 3		
PVA350-3.8	25	9.0 ± 0.5	2.7 ± 0.3		1.6 ± 0.4	9.7
PVA350-3.8	35	11 ± 1	2.8 ± 0.2		5.0 ± 1.0	23
PVA350-3.8	45	12.5 ± 2	3.1 ± 0.2		4.5 ± 0.5	75
PVA350-3.8	55	14 ± 1	3.4 ± 0.2		4.4 ± 1.0	140
PVA350-4.2	15	6.7 ± 0.4	2.8 ± 0.2	8.3 ± 1.5		
PVA350-4.2	25	8.8 ± 0.3	2.8 ± 0.1	33 ± 15		
PVA350-4.2	35	10 ± 1	3.1 ± 0.2	77 ± 40		
PVA350-4.2	45	12 ± 0.7	3.3 ± 0.3		1.3 ± 0.2	83
PVA350-4.2	65	18 ± 2	3.2 ± 0.3		5.5 ± 0.4	96
PVA350-4.5	15	6.3 ± 0.5	3.0 ± 0.15	10 ± 7		
PVA350-4.5	25	7.7 ± 0.3	3.2 ± 0.2	34 ± 9		
PVA350-4.5	35	10 ± 1	3.1 ± 0.1	77 ± 45		
PVA350-4.5	45	12 ± 1	3.2 ± 0.3		1.3 ± 0.4	26
PVA350-4.5	65	15 ± 2	3.5 ± 0.5		2.6 ± 0.4	160

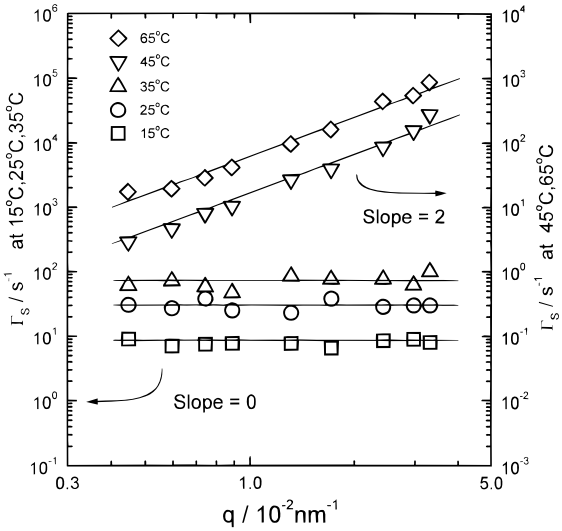

Figure 7. Scattering vector dependence of the decay rate Γ_s characteristic of the slow mode at five temperatures of T = 65, 45, 35, 25, and 10 °C from top to the bottom for the solution with C = 4.2 wt %.

order of 1 μm. There remains an intriguing problem what viscosity should be used for an estimate of R. In fact, use of solution viscosity is considered to give the smallest value among acceptable values of R. Relatively large R values are not inconsistent with that the dynamical correlation length ξ_H could be measured as the fast mode at these temperatures and strongly suggest that the solutions do not become molecular solutions immediately after they lost viscoelasticity, but a large concentration fluctuation persists up to higher temperatures. Eventually, there is no inconsistency between DVE and DLS results, and a clear boundary may be probably drawn for separating viscoelastic fluid and viscous fluid on the $T-C$ diagram.

Discussion

Viscosity Behavior. As already stated, η vs C curves for PVA/Borax samples with different molecular weights could be superposed to make one composite curve using the reduced concentration C/C_N. The C_N was demonstrated as the concentration at which viscous fluid suddenly transformed to uniform viscoelastic network. Some η vs T curves in Figure 5 enable us to locate the temperature T_N for each C as the inflection point in the corresponding curve to an accuracy of ±1 °C. Using T_N/T as the reduced variable instead of T, we successfully

Table 4. Relation between T_N and C

C/wt %	T_N/K	C/wt %	T_N/K
3.0	273	4.2	309
3.3	281	4.5	314
3.6	291	5.0	322
3.8	297	5.5	330
4.0	303	7.0	346

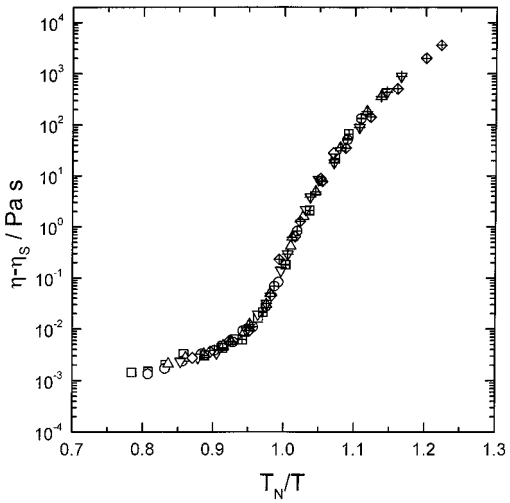

Figure 8. Steady viscosity $\eta - \eta_s$ at various C given in Figure 5 superposed by the horizontal shift alone using the reduced temperature T_N/T.

superposed those curves by the horizontal shift alone. Three curves for C = 3.0, 3.3, and 7.0 wt % were then superposed on to the reduced curve by shifting horizontally, from which T_N was estimated. Table 4 gives values of T_N for respective C. The viscosity data for $C \leq 2.0$ wt % were not used for this superposition procedure, simply because the samples did not show any viscoelasticity in the ω range measured. The results shown in Figure 8 indicate that all viscosity data ranging from 10^{-3} Pa s to nearly 10^4 Pa s can be well superposed on a curve with this quite empirical procedure.

We present a relation between T_N and C by a solid curve in Figure 9. This $T-C$ diagram distinguishes solutions according to their dynamical behaviors; i.e., temperatures at which solutions exhibited viscoelasticity are designated by filled circles and those at which solutions behaved as viscous fluid by unfilled ones. We see that the T_N-C curve lies just between two different dynamical behaviors and may be regarded as a boundary line between them. This may give a physical meaning to T_N along with C_N as characteristic param-

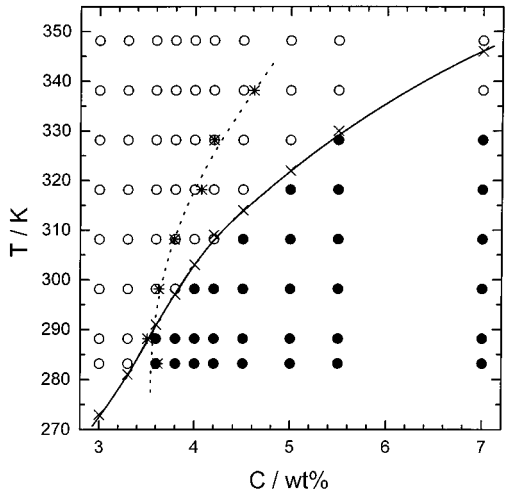

Figure 9. T_N used for reduction of steady viscosity data plotted against C. The T_N-C curve is drawn in the figure as the solid curve by interconnecting T_N values (×) determined at respective C values. It forms a boundary line to distinguish solutions according to two different dynamical behaviors: temperature at which solutions exhibited viscoelasticity are designated by filled circles and those at which solutions behaved as viscous fluid by unfilled ones. The dotted line represents a change in overlapping concentration C^* of the PVA sample with T.

eters for discussing association behaviors of PVA in aqueous Borax solution. Stated in another way, if an experiment is done at constant temperature of T_1 for solutions with varying C, the value of C_N obtained may be equal to that at the intersection point between the T_N-C curve and the straight line at $T = T_1$ drawn in parallel to the abscissa.

It should be remarked upon that the above conjecture may not hold at a higher temperature where complicated interactions of Borax with PVA chains in water begin to affect structure and dynamics of the system in a different way as described in Introduction. Indeed, the solution with $C = 7.0$ wt % became a viscous fluid below T_N. Static light scattering experiments have shown that scattering intensity $I(q)$ of this solution is low at room temperature and scarcely dependent on the scattering angle, while it gradually increases with time at 65°C, especially at low scattering angles. The phenomena has been found to occur in a thermoreversible fashion. Results of detailed investigations on the anomalous time evolution of $I(q)$ shall be reported in a forthcoming paper. Thus, it should be kept in mind that the treatment may be valid in a T range where reproducible data are obtained during some time interval, e.g., at least 1 h, during which our DVE measurements were conducted.

In the figure, a variation of C^* with T is also shown by the dotted line, which intersects the T_N-C curve at around $C = 3.6$ wt %. If an estimate of C^* from intrinsic viscosity measurements is adequate, chain overlapping is likely to be a necessary condition for formation of a viscoelastic network but a sufficient number of the didiol complexes is needed for maintaining the network. We concluded in the earlier paper[4] that C_N was very close to C^* at 25 °C. The conclusion now turns out to be valid only around room temperature.

Elastic Behavior. The number of elastically effective chains ν_{eff} is presumably related to the number of didiol complexes. Preliminary ^{11}B NMR experiments have been performed for the PVA/Borax solution with $C =$ 4.5 wt % to obtain an equilibrium constant K_2 for the following chemical reaction.[21]

$$2A + B^- \rightleftharpoons A_2B^- + 4H_2O \qquad (4)$$

The symbols A, B^-, and A_2B^- represent free PVA, monoborate, and PVA/monoborate complex, i.e., the didiol complex, respectively. Since we prepared the solution with a weight ratio of PVA:SB = 2:1, the same as that used for DVE and DLS measurements, a fairly large amount of boric acid was present and the NMR spectroscopy detected a considerably large peak due to polyborate. Overlapping of this peak on that assigned to the didiol complex resulted in an inaccurate determination of K_2. A ratio of $[A_2B^-]$ to the number of PVA chains ν both expressed in units of mol/nm^3 was slightly larger than unity over a T range from 30 to 60 °C and became less than unity at higher T. The temperature dependence of K_2 followed the Arrhenius type equation in the low T range, from which the activation energy ΔH was calculated as 21 ± 5 kJ/mol. This value may be compared with values of ΔH calculated from ν_{eff} data given in Figure 5 by assuming the Arrhenius type of T dependence. We obtained $\Delta H = 18 \pm 1$ kJ/mol for $C =$ 7.0 wt % and $\Delta H = 32 \pm 2$ kJ/mol for other C on average. To the same PVA/Borax system, Schulz and Myers[14] reported $\Delta H = 21$ kJ/mol from analysis of dynamic mechanical data, and Sinton[6] gave a little larger value of $\Delta H = 35$ kJ/mol for T dependence of K_2 calculated from ^{11}B NMR spectroscopy. Two ΔH values obtained from T dependence of K_2 and ν_{eff} for our sample are in fairly good agreement with values in the literature.

According to eq 4, the number of didiol complexes is proportional to the square of polymer concentration. Those complexes are used for formation of clusters through association of PVA chains in the low C region, and a part of them becomes elastically effective only after C exceeds C_N at a fixed T. We have shown that all ν_{eff}/ν data estimated for PVA samples with five different molecular weights at 25 °C are superposed on a curve in the plot of ν_{eff}/ν against $(C - C_N)/C_N$, and suggested that C_N should be regarded as a kind of the gel point at which ν_{eff} is zero.[4] We have postulated that the T_N-C curve permits us to estimate C_N of PVA solutions at any desired temperature unequivocally. If this postulate is really applicable, we may consider that ν_{eff}/ν of a solution with $C = C_1$ at $T = T_1$ can be treated as a unique function of $(C_1 - C_{N,1})/C_{N,1}$ where $C_{N,1}$ is the threshold concentration at $T = T_1$, being easily read from the T_N-C curve. Changes in ν_{eff} with T^{-1} given in Figure 5 were converted to changes in ν_{eff} with corresponding difference in polymer concentration, $C - C_N$, and results are logarithmically plotted in the form of ν_{eff}/ν vs $(C - C_N)/C_N$ in Figure 10. Rather surprisingly, all data are well superposed on the smooth curve obtained in an earlier study[4] where growth of viscoelastic networks with C has been investigated. A group of curves drawn in Figure 10 are predictions of a statistical−mechanical theory for elastically effective chains in transient gels developed by Tanaka and Ishida.[22] The theory qualitatively agrees with experiments and reasons for discrepancy were discussed in detail.[4] The success in superposition gives a strong support to our interconversion scheme for unified description of T and C dependencies of ν_{eff}/ν and leads to the conclusion that T_N may be regarded as a kind of sol−gel transition temperature for this PVA/Borax system.

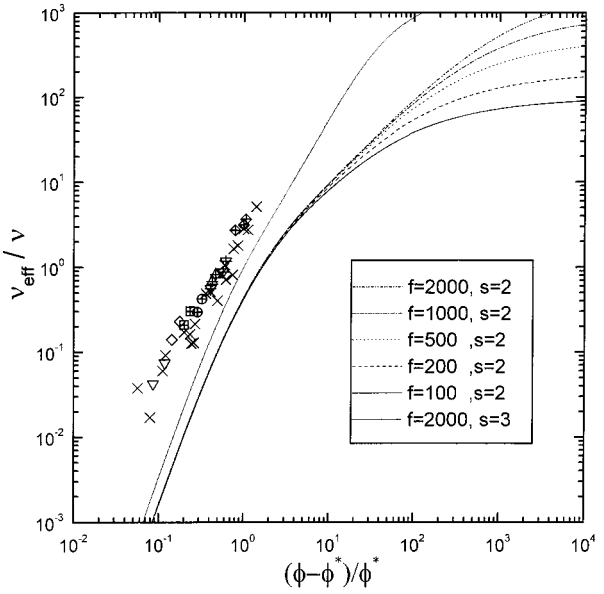

Figure 10. Temperature dependence of the reduced number of elastically effective chains ν_{eff}/ν converted to concentration dependence of ν_{eff}/ν, using the scheme described in text, and plotted against $(C - C_N)/C_N$. Earlier data[4] are given by symbols (×) and the symbols for the samples studied in this work are the same as in Figure 3. A group of curves are theoretical predictions for ν_{eff}/ν in transient gels.[22]

Time−Concentration Reduction. Composite curves were successfully constructed at each C from DVE data at different temperatures based on the time−temperature superposition principle. We applied the time−concentration reduction scheme to those composite curves choosing the curve with $C = 4.5$ wt % as the reference one. First, the curves obtained at other C ranging from 3.8 to 7.0 wt % were vertically shifted so that their plateau moduli G_N may coincide with that of the reference curve, respectively, and then shifted horizontally. The result is shown in Figure 11. Whole G' and G'' data are nicely superposed to give one master curve except G'' data at the high ω end. Data scattering of G' at the low ω end may be ascribed to experimental difficulties for determining small G' values with our apparatus. From the success of the time−concentration reduction procedure, we may conclude that the relaxation process is governed by the same molecular mechanism over the whole range of C and T studied, presumably by dissociation−association kinetics of diol complexes accompanied by the interchain dynamics.

Acknowledgment. The authors are grateful to Prof. I. Ando and his group for having performed ^{11}B NMR experiments. We also thank Kuraray Co. Ltd. for a gift of the PVA sample. This work was supported in part by a Grant-in-Aid for Scientific Research, the Ministry of Education, Science, and Culture, Japan (Grant-in-Aid10305070).

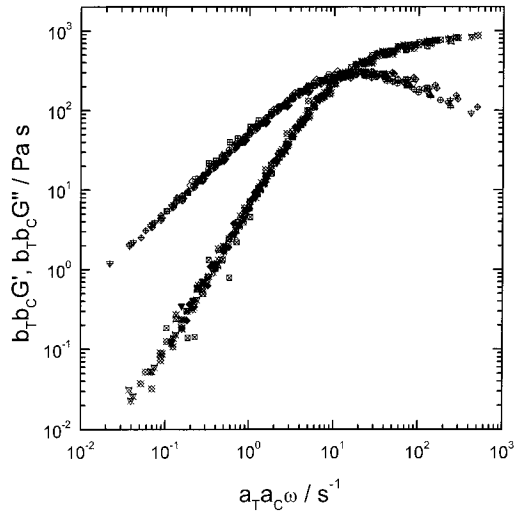

Figure 11. Application of the time−concentration reduction scheme for construction of one master curve which systematically describes the dynamical aspects of PVA350 in aqueous Borax solution over the entire ranges of T and C studied. The reference concentration is 4.5 wt %. Symbols are the same as in Figure 3.

References and Notes

(1) Koike, A.; Nemoto, N.; Inoue, T.; Osaki, K. *Macromolecules* **1995**, *28*, 2339.
(2) Nemoto, N.; Koike, A.; Osaki, K. *Macromolecules* **1996**, *29*, 1445.
(3) Takada, A.; Nemoto, N. *Prog. Colloid Polym. Sci.* **1997**, *106*, 183.
(4) Takada, A.; Nishimura, M.; Koike, A.; Nemoto, N. *Macromolecules* **1998**, *31*, 436.
(5) Shibayama, M.; Sato, M.; Kimura, Y.; Fujiwara, H.; Nomura, S. *Polymer* **1988**, *29*, 336.
(6) Sinton, S. W. *Macromolecules* **1987**, *20*, 2430.
(7) Pezron, E.; Leibler, L.; Lafuma, F. *Macromolecules* **1989**, *22*, 2656.
(8) Pezron, E.; Ricard, A.; Lafuma, F.; Audebert, R. *Macromolecules* **1988**, *21*, 1121.
(9) Pezron, E.; Leibler, L.; Ricard, A.; Lafuma, F.; Audebert, R. *Macromolecules* **1989**, *22*, 1169.
(10) Wilson, M. E.; Najdi, S.; Krochta, J. M.; Hsieh, Y.-L.; Kurth, M. J. *Macromolecules* **1998**, *31*, 4486.
(11) Sato, T.; Tsujii, Y.; Fukuda, T.; Miyamoto, T. *Macromolecules* **1992**, *25*, 3890.
(12) Ide, N.; Sato, T.; Miyamoto, T.; Fukuda, T. *Macromolecules* **1998**, *31*, 8878.
(13) Ferry, J. D. *Viscoelastic Properties of Polymers*; John Wiley: New York, 1980.
(14) Schulz, R. K.; Nyers, R. R. *Macromolecules* **1969**, *2*, 281.
(15) Nemoto, N.; Makita, Y.; Tsunashima, Y.; Kurata, M. *Macromolecules* **1984**, *17*, 2629.
(16) Brown, W.; Nicolai, T. In *Dynamic Light Scattering−The Method and Some Applications*; Brown, W. Eds.; Oxford University Press: Oxford, England, 1993; Chapter 6.
(17) Shibayama, M.; Kurokawa, H.; Nomura, M. *Polymer* **1992**, *33*, 2883.
(18) Brochard, F.; de Gennes, P. G. *Macromolecules* **1977**, *10*, 1157.
(19) Brochard, F. *J. Phys. Fr.* **1983**, *44*, 39.
(20) Doi, M.; Onuki, A. *J. Phys. II Fr.* **1992**, *2*, 1631.
(21) Nemoto, N.; Koga, K.; Takada, A.; Ando, I. To be published.
(22) Tanaka, F.; Ishida, M. *Macromolecules* **1996**, *29*, 7571.

MA990493W